American Mineralogist, Volume 76, pages 60–73, 1991

Structural analysis of radiation damage in zircon and thorite: An X-ray absorption spectroscopic study

François Farges, Georges Calas

Laboratoire de Minéralogie-Cristallographie, Universités Paris 6 et 7, CNRS UA09, Tour 16/2, 4 Place Jussieu, 75252 Paris Cedex 05, France

Abstract

Metamictization effects have been investigated in zircon, thorite, uranothorite, and thorogummite using X-ray absorption spectroscopy at Zr-*K*, Th-L_{III}, and U-L_{III} edges. Extended X-ray absorption fine structure (EXAFS) spectra of metamict samples are characterized by a major contribution due to the O nearest neighbors with some contributions from next-nearest neighbors (Si and Zr in zircon, Si in thorite). In zircon, Zr-O distances decrease by ≈0.1 Å while the coordination number of Zr decreases from 8 to 7. In contrast, the eightfold coordination of Th in crystalline thorite is preserved in metamict thorite. Si second neighbors around Zr or Th are generally observed in metamict samples with distances close to those measured in crystalline phases. No other contribution to EXAFS is observed in thorite, but Zr-Zr distances are observed in zircon. They decrease by ca. 0.3 Å as a function of zircon metamictization. Minor elements have been studied in one metamict zircon (Näegi, Japan): Hf and Th are eightfold coordinated whereas unusual sixfold coordinated U(IV) is observed. The location of the actinide polyhedra in metamict and annealed zircon cannot be precisely characterized with the available EXAFS data. In the thorite samples investigated, U occurs as uranyl groups which often contribute to a bright color ("orangite").

Metamictization processes are characterized by a loss of medium range order. There is no evidence for decomposition into crystalline oxides. Furthermore, metamict and glassy silicates do not exhibit the same local structure around Zr and Th. The structural interpretation of EXAFS data must take into account the creation of O vacancies arising from a displacement or tilting of the SiO_4 tetrahedra during metamictization of zircon-like structures. If the cation can take a lower coordination number (as in the case of Zr), a coordination change allows the local structure to be partly maintained during metamictization. If not, as for Th, the local structure is rapidly destroyed. Significant weathering is responsible for the presence of U as uranyl complexes in metamict thorium silicates, probably enhanced by radiation damage. Intense weathering is also responsible for the decomposition of thorogummite into simple oxides.

Introduction

Phase transitions from a periodic to an aperiodic structure occur in various minerals as a result of severe radiation damage induced by alpha-radiation and recoil nuclei accompanying the decay of the actinides they contain. Complex oxides and zircon-group silicates are the most common metamict minerals. Considerable structural and chemical data have been obtained because of the interest in radioactive dating and nuclear waste disposal of high activity elements (Harker and Flintoff, 1985; Chakoumakos et al., 1987; Ewing et al., 1987). The disordered structural state of metamict samples greatly limits diffraction-based methods, which can be used for studying the first stages of metamictization. Indeed, modifications observed in the physical properties (e.g., density, elastic properties, or sound velocity) are difficult to correlate with the structural transformations which lead to a fully metamict state. It is thus necessary to use a method sensitive to short-range structure such as X-ray absorption spectroscopy (XAS). This method has been extensively used in the determination of the local structure of a wide range of glasses and disordered minerals (Brown et al., 1988; Calas et al., 1987). XAS has been used in the study of various $A_xB_yO_z$ metamict oxides (Greegor et al., 1984, 1985a, 1985b, 1986, 1987; Lumpkin et al., 1986) but it has been only recently applied to metamict silicates, and only zircon has been qualitatively investigated (Barinsky and Kulikova, 1977; Nakai et al., 1987). The interest in zircon metamictization arises from its possible influence on discordant age determinations in U-Th-Pb age dating. The structural modifications which occur in the metamict state also affect the behavior of zircon and thorite during alteration and weathering. Finally, the local structure of these amorphous silicates, which result from a solid-state

0003–004X/91/0102–0060$02.00

transformation induced by radiation, may be compared to that in quenched Zr-, Th-, and U-bearing silicate melts (Farges, 1989).

Zircon and thorite crystallize in space group $I4_1/amd$ (Hazen and Finger, 1979; Taylor and Ewing, 1978). Their structures can be described as consisting of chains of alternating edge-sharing SiO_4 tetrahedra and MeO_8 (Me = Zr or Th) triangular dodecahedra extending parallel to [001] and linked by edge-sharing MeO_8 polyhedra. In the absence of annealing, metamictization is related to the age (in the Ga range) or the presence of a high actinide content (ca. in the 1000 ppm range or more: Holland and Gottfried, 1955; Murakami et al., 1986; Chakoumakos et al., 1987). Crystalline and metamict zircon have long been referred to as "high zircon" and "low zircon," respectively. The latter exhibits lower values of such parameters as density, refractive index, and birefringence (Holland and Gottfried, 1955). The metamict state of zircon is usually determined through X-ray diffraction (XRD) patterns (Pabst, 1952; Holland and Gottfried, 1955; Murakami et al., 1986). More detailed investigations of metamict zircon have involved diffuse X-ray scattering (Vance and Anderson, 1972; Sugiyama and Waseda, 1989) and high resolution transmission electron microscopy (HRTEM: Yada et al., 1981; Headley et al., 1981; Chakoumakos et al., 1987; Yada et al., 1987). Those studies rule out decomposition to simple oxide components and show the presence of amorphous and crystalline domains. Infrared spectroscopy has indicated the presence of some amorphous silica (Hubin and Tarte, 1971, 1974; Vance, 1975) and the importance of hydroxyl groups (Aines and Rossman, 1985, 1986; Caruba et al., 1985).

In contrast to zircon, thorite occurs primarily in the metamict state. As Zr and tetravalent actinides have distinctly different ionic radii, thorite often has a larger U content than zircon. Uranothorite, for example, represents partial solid solution between thorite and coffinite $USiO_4$ (Fuchs and Gebert, 1958; Zimmer, 1986). However, in some natural uranothorite, uraninite inclusions may enhance the apparent U content (Robinson and Abbey, 1957; Staatz et al., 1976) and special care is necessary before any spectroscopic investigation is undertaken. No data exist regarding the oxidation state of U in natural metamict uranothorite (Speer, 1982), but it is usually assumed to be hexavalent (Lumpkin and Chakoumakos, 1988). Finally, hydrous thorium silicates are referred to as thorogummite (Frondel, 1953).

The crystal chemistry of minor components cannot be determined without specific spectroscopic data (see Hawthorne, 1988). In zircon, the state of U can be investigated by optical absorption spectroscopy and it occurs essentially in the tetravalent state, although pentavalent U is also known (Richman et al., 1976; Vance, 1974, 1975; Vance and Mackey, 1975; Mackey et al., 1975; Vance et al., 1980). Some difficulties are encountered in deriving the symmetry of the site occupied by U ions, because crystal field components cannot be directly obtained in $5f^n$ systems (Calas, 1979). Among the other minor components, large concentrations of Hf are found in zircon due to the solid solution between zircon and hafnon (Correia Neves et al., 1974). The relation between Hf content and metamictization has been examined because the large value of the alpha–cross section of Hf (115 compared to 0.18 for Zr) would cause the susceptibility of zircon to metamictization to increase (Speer and Cooper, 1982). This effect is reinforced by the fact that Hf and actinide content are positively correlated in natural samples (Holland and Gottfried, 1955; Speer, 1982).

We present in this study a systematic analysis of XAS spectra at the Zr-K edge and the Hf-, Th-, and U-L_{III} edges, for zircon and thorite samples spanning the range of alpha-decay doses over the crystalline to metamict transition. The local structure around atoms of these elements has been determined as a function of the increasing alpha-decay dose estimated from XRD patterns. The spectacular transition observed in the evolution of local structures during metamictization gives new insight into the structural mechanisms which control the transformation.

Sample selection and characterization

Zircon

A synthetic zircon sample grown by Hautefeuille in a sodium molybdate flux at 1250 °C (Hautefeuille and Perrey, 1888) has been used as a standard. An estimate of the crystallinity of natural samples is given by the ratio $\mathscr{R}$ between the observed intensity (including the diffuse scattering component) of the 200 reflection of the studied sample to that of synthetic zircon (Table 1). The 200 peak is used because most other reflections rapidly become unobservable at high alpha-doses. However, XRD must be used with caution in studies of metamict samples because the contribution of diffuse scattering is larger than the Bragg component (Murakami et al., 1986). $\mathscr{R}$ ranges between 1 and nearly 0.20 for the crystalline zircon samples investigated. Partly metamict zircon has an $\mathscr{R}$ parameter ranging from 0.10 to 0.01 whereas for totally metamict zircons, $\mathscr{R}$ is lower than 0.01 (Table 1). The alpha-event dose was calculated from ^{238}U and ^{232}Th contents by considering the published age, in the absence of any known natural annealing (Table 1).

Ten different zircon samples were selected from an initial collection of nearly 45 samples. Zircon samples that had been annealed for gemological purposes or containing baddeleyite inclusions were rejected. Euhedral crystalline zircon has been found in a carbonatite (Mud Tanks, Alice Springs, Australia) and in an unaltered pegmatite (Diamantina, Brazil). Green detrital zircon samples from Miask (Ural Mountains, U.S.S.R.) came from carbonatites and related rocks (miaskites) of the Il'menogorsky-Vishnevogorsky alkaline complexes. U/Pb data give an age of 0.42–0.32 Ga (Chernyshev et al., 1987) for those samples. The zircon samples from Betafo (Ambatofotikety) and Ampagabe, Madagascar (labeled cyrtolite) were

TABLE 1. Sample identification

Sample origin	Sample number*	Color	Ratio $\mathscr{R}$	a (Å)	α-dose/mg**	Age (in Ga)
		Zircon				
Synthetic		translucent	[reference]	6.604(4)	—	—
Mud Tanks, Australia	SORB no. 8438	orange	0.63	6.604(4)	—	—
Diamantina, Brasil	$ZIR no. 07	brown	0.26	6.604(4)	—	—
Miask, Ural Mountains, U.S.S.R.	SORB no. 7121	green	0.07	6.630(4)	0.2	0.42–0.32
Betafo, Madagascar	SORB no. 8676	brown	0.04	6.674(8)	3	1.65–0.5
Ampagabe, Madagascar	SORB no. 8221	brown	0.03	6.674(8)	3	1.65–0.5
Hitterö, Norway	ENSMP no. 19391	white	0.02	6.670(8)	2	1.64–0.9
Näegi no. 1, Mino, Japan	ENSMP no. 19419	gray-green	0.02	6.674(8)	2	0.125
Näegi no. 2, Mino, Japan	ENSMP no. 19419	dark green	totally metamict†	—	4	0.125
Sri Lanka	MNHN‡	green	totally metamict	—	0.5	0.56
Kinkle's Quarry, New York, U.S.A.	MNHN no. 2432C	brown-black	totally metamict	—	6	0.3–0.35
		Thorite				
Synthetic		translucent	[reference]	3.565(4)	—	—
Ambatofotsy, Madagascar	SORB no. 7229	yellow	0.02	3.542(8)	20	1.65–0.5
Andranomitroky, Madagascar	SORB no. 8616	yellow	0.01	3.540(8)	20	1.65–0.5
Madagascar (unknown location)	SORB no. 7221	brown	0.01	3.542(8)	30	1.65–0.5
Brevik, Norway	ENSMP‡	black	totally metamict†	—	50	1.64–0.9
		Uranothorite				
Arendal, Norway	SORB no. 7224	brown	0.010	3.535(8)	80	1.64–0.9
Svenes, Norway	ENSMP‡	brown	totally metamict†	—	70	1.64–0.9
Tvegestrand, Norway	MNHN‡	yellow	totally metamict	—	100	1.64–0.9
		Thorogummite				
Andranomitroky, Madagascar	SORB no. 8616	pale yellow	0.015	3.558(8)	20	1.64–0.9
Iazaka, Fukushima, Japan	SORB no. 8577	pale yellow	0.010	3.542(8)	—	—

* Original collection: SORB = Collection de la Sorbonne (Laboratoire de Minéralogie-Cristallographie), Paris. ENSMP = Ecole Nationale Supérieure des Mines de Paris. MNHN = Museum National d'Histoire Naturelle, Paris. $ = personal collection of the authors.

** Cumulative α-dose in 10^{16} α/mg.

† $\mathscr{R} < 0.01$.

‡ No identification number.

found in a U-rich pegmatite with other metamict minerals such as bastnaesite or davidite (Lacroix, 1921–1923). They are 1.65 Ga old but a metamorphic event occurred near 0.5 Ga (Besairie, 1970). The zircon samples from Hitterö (Norway) occur as pale, zoned doubly terminated crystals extracted from a charnockitic granite dated to the Scoronorwegian event of the Scandinavian shield (ranging between 1.64 and 0.9 Ga old: Field et al., 1985). Green zircon from Sri Lanka originated in stream deposits and has been studied by various authors (Holland and Gottfried, 1955; Murakami et al., 1986; Chakoumakos et al., 1987). Totally metamict and highly weathered zircon (radioactive cyrtolite) from Kinkle's Quarry (Westchester County, New York) is associated with uranthorite in pegmatites of the Bedford complex (Alavi, 1976). Metamict zircon is also found in the Ebisu mine, Näegi (Takayama Prefecture, Mino, Japan) associated with thorite in the stream bed of a Pleistocene continental placer. That zircon has been described as occurring in a nearby, late Cretaceous pegmatite (Takabatake, 1962). Some single crystals (1 cm) are only slightly weathered and zoned. In contrast to previous studies (Nagashima and Nagashima, 1960; Nakai et al., 1987; Sugiyama and Waseda, 1989), we have found that these zircon crystals show large variations in alpha-decay damage, related to important variations in the total actinide content (between 2 and 20 wt%: Table 2). Two samples have been subsequently selected (Näegi no. 1 and no. 2) to account for the variations encountered in specimens from this locality. No significant amounts of P were detected in any zircon, and epitaxial overgrowths of xenotime are thus not likely.

Thorite and uranothorite

Synthetic thorite (α-$ThSiO_4$) has been grown by M. P. Lahalle (Institut de Physique Nucléaire, Orsay, France) in a $LiMoO_4$-MoO_3 flux at 1200 °C according to the procedure of Chase and Osmer (1966). Thorite from Norway occurs in the same geological surrounding as Hitterö zircon and is found in various locations in the southern Norwegian shield including Langesundfjord (Lövö island, Brevik), Arendal and nearby occurrences (Landbö, Tvegestrand, Svenes). The majority of samples do not diffract X-rays, especially when the U content is greater than 4 wt% (Table 3). Some thorite from Madagascar comes from the Ambatofotsy amphibolitic gneiss in association with "uranothorianite," betafite and metamict zircon. Its age is similar to that of the Betafo zircon (1.65–0.5 Ga). All samples show evidence of weathering, including secondary complex Th, U, Ti, Pb oxides in fractures; Th depletion and Ca enrichment from the core of the rim of crystals and, finally, significant H_2O contents. In some samples (Madagascar), annealing has occurred.

Metamict thorite exhibits large compositional ranges (Table 3), with some unusual components (up to 2 wt% MnO component in the Brevik thorite). The large amount of P in Madagascar thorite no. 7221 did not correlate

TABLE 2. Chemical analyses of metamict zircon

	Miask, U.S.S.R.	Ampagabe, Madagascar	Hitterö, Norway	Sri Lanka ($\rho = 4$ g/cm³)	Kinkle's Quarry, U.S.A.	Näegi no. 1, Japan	Näegi no. 2, Japan
SiO_2	32.15	19.80	30.80	32.35	25.90	27.80	25.60
ZrO_2	63.75	56.75	64.40	64.30	49.55	53.90	41.60
P_2O_5	0.00	0.50	0.01	0.00	0.40	1.05	0.20
CaO	0.00	0.80	0.25	0.00	1.55	0.00	0.25
FeO	0.00	1.90	0.50	0.00	0.85	0.05	0.00
MnO	0.00	0.05	0.25	0.00	0.55	0.00	0.10
Y_2O_3	0.25	0.80	0.70	0.00	0.85	1.65	0.15
Ta_2O_5	—	—	0.10	—	—	1.10	1.00
HfO_2	1.60	4.70	2.10	1.35	7.10	4.60	8.15
UO_2	0.20	1.85	0.35	0.30	5.60	4.70	8.25
ThO_2	0.05	1.35	0.10	0.05	0.05	2.85	10.55
PbO	0.10	0.20	0.00	0.05	0.10	0.05	0.05
Σ	98.10	99.80	99.65	98.30	92.50	97.75	95.90
H_2O	0.50	0.20	—	—	7.10	2.00	5.20
[by the Penfield method (±0.10)]							

Note: Experimental conditions for microprobe analyses: 15 kV, 5 mA, spot size: 4 μm. Reference standard in { } for each set of counting time: P{apatite}, Si{anorthite 0.96}, Al{albite}, Mg{diopside}, Fe{Fe_2O_3}, Zr{zircon}, Y{$YNbO_3$}, Hf[0.2]{HfO_2}, Th[ThO_2]{0.5}, U[UO_2]{0.5}: 5 s. S{PbS}, Ca{anorthite 0.96}, Ti{$MnTiO_3$}, Mn{$MnTiO_3$}, Ta{Ta_2O_5}, Nb{$YNbO_3$}, Pb{PbS}, Ce{Ce_2O_3}: 10 s. Mean values for eight to 15 point analyses.

TABLE 3. Chemical analyses for metamict thorite, uranothorite, and thorogummite

	Brevik ENS-MP	Ambatofotsy no. 7229	Madagascar no. 7221	Svenes ENS-MP	Arendal no. 7224	Tvegestrand no. 7232	Andranomitroky, Madagascar no. 8616 (core*)	Andranomitroky, Madagascar no. 8616 (rim**)
SiO_2	20.25	20.50	5.90	15.30	16.25	15.35	22.20	20.45
ThO_2	61.90	60.05	63.75	52.25	52.15	53.25	44.35	34.50
UO_2	1.30	1.70	4.15	7.90	10.25	14.90	1.65	2.05
P_2O_5	0.00	3.20	9.60	1.10	2.30	0.35	2.00	2.20
S	0.00	0.00	0.00	0.00	0.20	0.00	2.15	1.70
CaO	2.30	6.20	0.45	1.30	1.65	2.75	4.20	6.80
MgO	0.00	0.00	0.00	0.00	0.00	0.00	0.15	0.30
Fe_2O_3	1.65	0.20	4.60	9.90	6.25	0.10	0.65	0.25
MnO	2.45	0.05	0.00	0.00	0.00	0.00	0.00	0.00
ZrO_2	0.15	0.50	0.05	0.00	0.00	0.10	0.00	0.25
Y_2O_3	0.20	0.50	0.00	0.00	1.80	0.00	0.00	0.00
Ce_2O_3	0.20	0.00	0.10	0.05	0.10	0.05	3.45	3.50
PbO	0.00	0.50	3.70	0.20	1.35	1.45	2.15	1.70
Σ	90.40	93.40	92.30	88.00	94.40	88.30	82.95	73.75
H_2O	10.30	8.40	8.00	11.20	9.50	11.80	7.70	16.55
[by the Penfield method (±0.10)]								

* Core = primitive thorite.
** Rim = surrounding thorogummite.

with REE or Ca content, thus excluding monazite inclusions. The U content of uranothorite ranges from 1.68 to 14.9 wt% UO_2 (no. 7229 from Madagascar and no. 7232 from Norway).

Thorogummite

Thorogummite is described as a complex thorium hydrous silicate (Frondel, 1953) and it forms from various primary Th and U phases (both silicates and oxides). We have selected a sample from Iazaka, Fukushima Prefecture, Japan (Iimori and Hata, 1938) which resulted from the weathering of metamict thorian yttrialite, and another sample sorted from the rim surrounding an orange metamict thorite sample (Andranomitroky, Madagascar). Thorogummite contains minor ThO_2 as detected by XRD. Penfield analyses show a higher H_2O content in the thorogummite compared to that in the thorite (Table 3). Further differences include decreasing Th- and increasing Ca-content from the core (original thorite) to the rim (thorogummite).

EXPERIMENTAL

Chemical analyses were performed using a Cameca microbeam electron microprobe, using the experimental conditions summarized in Table 2. The total H_2O content was measured using the Penfield gravimetric method. Annealing experiments were carried out on powdered samples in a Pt crucible for 3 h in air. XRD patterns were recorded on a Philips PW 1740 powder diffractometer (Cu$K\alpha$ radiation) operated at 35 kV and 30 mA. Powdered quartz from Madagascar was used as an internal standard and all diffraction patterns were recorded with a long counting time (100 s/0.02° 2θ) in order to ensure a high signal/noise ratio. For U-containing samples, optical absorption spectra were measured between 30000 and 4000 cm^{-1} on a Cary 2300 spectrophotometer. Diffuse reflectance spectra were obtained using powdered samples and were transformed into absorbance-equivalent spectra using the Kubelka-Munk formalism (Wendlandt and Hecht, 1966).

XAS spectra were obtained in transmission mode at the Zr-K edge (17998 eV) and at the L_{III} edge for Hf (9876 eV), Th (16299 eV), and U (17163 eV) using the LURE/DCI synchrotron source (Orsay, France). The ring was operating at 1.85 GeV with an injection current of 250–300 mA. The energy was calibrated at 17998 eV using the first maximum of metallic Zr, with a two-crystal Si(311) monochromator. Spectra were recorded from 150 eV below to 1000 eV above the absorption edge energy, and two of ten spectra were obtained and averaged for each sample in order to improve the signal to noise ratio. Core hole effects and experimental broadening effects give an overall energy resolution of 3.5 eV at 18000 eV. Special care was taken in sample preparation in order to avoid spurious absorbance. After grinding in V27 Rhodorsil oil (to avoid U-leaching), powders were dispersed with ultrasonic methods and the fraction smaller than 20-μm was selected to reduce the maximum grain size to a fraction of sample thickness. The powder was deposited on micropore-type filters with a thickness ranging from 60 μm to 90 μm depending on actual sample composition.

Two kinds of data may be extracted from XAS spectra. The X-ray absorption near edge structure (XANES) gives

Table 4. Table of crystalline compounds used for Zr data reduction

Compound	EXAFS results	Structure refinement data	References
Zr-O*			
Elpidite (Mont St.-Hilaire, Canada)	6.0 × O at 2.08 Å (0.00)	6 × O at 2.076 Å (0.097)	Cannillo et al., 1973
Catapleite (Mont St.-Hilaire, Canada)	6.0 × O at 2.07 Å (0.00)	6 × O at 2.073 Å (0.005)	Illyushin et al, 1981
Baddeleyite (synthetic)	7.0 × O at 2.17 Å (0.08)	7 × O at 2.17 Å (0.08)	Smith and Newkirk, 1965
Zircon (synthetic)	8.0 × O at 2.20 Å (0.06)	8 × O at 2.205 Å (0.06)	Hazen and Finger, 1979
Uncertainties estimated for Zr-O: ±0.5 for CN; ±0.01 Å for R and $\Delta\sigma$			
Zr-Si**			
Elpidite	10.0 × Si at 3.67 Å (0.10)	6 × Si + 4 × Na at 3.60 Å (0.06)	Cannillo et al., 1973
Catapleite	12.0 × Si at 3.64 Å (0.10)	6 × Si + 6 × Na at 3.65 Å (0.07)	Illyushin et al., 1981
Zircon	2.0 × Si at 2.98 Å (0.02)	2 × Si at 2.99 Å (0.00)	Hazen and Finger, 1979
	3.8 × Si at 3.66 Å (0.04)	4 × Si at 3.64 Å (0.00)	Hazen and Finger, 1979
Uncertainties estimated for Zr-Si: ±1.0 for CN; ±0.03 Å for R and $\Delta\sigma$			
Zr-Zr**			
Baddeleyite	7.2 × Zr at 3.42 Å (0.09)	7 × Zr at 3.47 Å (0.07)	Smith and Newkirk, 1965
Zircon	4.0 × Zr at 3.64 Å (0.04)	4 × Zr at 3.64 Å (0.00)	Hazen and Finger, 1979
Uncertainties estimated for Zr-Zr: ±1.0 for CN; ±0.03 Å for R and σ			

Note: Structural data are as follows: coordination number, distance, and in parenthesis: statistical variation for crystalline samples or absolute Debye-Waller factor for parameters extracted with theoretical functions or relative Debye-Waller factor for parameters extracted from the corresponding reference.

* $BaZrO_3$ data: 6 × O at 2.095 Å (Berthet, 1987, personal communication).

** McKale data (McKale et al., 1988).

information on the geometry of the site and oxidation state of the absorbing element, and the extended X-ray absorption fine structure (EXAFS) gives structural information (e.g., interatomic distances, coordination number) near the absorbing element (Brown et al., 1988; Teo, 1986). The normalized, k^3-weighted EXAFS spectra (k represents the wave vector of the photoelectron) is analyzed via the Fourier transform (FT). The modulus of the Fourier transform shows the various atomic shells around the absorbing atom contributing to EXAFS. Structural parameters are obtained by curve-fitting analysis of the inverse Fourier transform of single peaks of the FT. Reference-derived and calculated (Teo and Lee, 1979; McKale et al., 1988) phase-shift and amplitude functions have been tested on various crystalline compounds, including strongly distorted cation environments. Reference compounds have been used to extract amplitude and backscattering phase-shift functions and also to test to the transferability of these functions to other reference compounds (Tables 4, 5, and 6 for Zr, Th, and U, respectively).

The coordination numbers derived from EXAFS are dependent on disorder effects which are important in aperiodic compounds. An harmonic approximation may be chosen in the case of a small radial disorder (Eisenberger and Brown, 1979). A Debye-Waller-like term is defined as: $\exp(-2\sigma^2k^2)$, where σ represents the Debye-Waller factor (including static and thermal contributions). However, σ describes the variation in the separation between the central and backscattering atoms, and not the deviations from their mean crystalline positions as in XRD. When experimental references are chosen instead of theoretical functions, $\Delta\sigma$/reference has the significance of a relative disorder term, with respect to the mentioned reference. Furthermore, non-Gaussian asymmetric distance distribution fits were calculated assuming a modified version of the model of de Crescenzi et al. (1981). No major changes were found between Gaussian and asymmetric distance distribution models, and the EXAFS structural parameters have been obtained in the harmonic (Gaussian) approximation model.

Results

Local structure around Zr in metamict zircon

Crystalline zircon. Interatomic distances obtained from data reduction (Table 4) are in good agreement with structure refinement based on XRD data (Hazen and Finger, 1979). The first peak of the FT (Fig. 1) arises from the Zr-O contributions: four O atoms near 2.13 Å and four others at 2.27 Å. The most intense peak corresponds to four Si and four Zr atoms at 3.64 Å, a distance which corresponds to edge-shared ZrO_8-ZrO_8 and corner-shared SiO_4-ZrO_8 polyhedra. A weak contribution from Si neighbors is found at 2.99 Å, corresponding to two edge-shared SiO_4-ZrO_8 polyhedra. The remaining shells at distances greater than 4.90 Å have not been analyzed although their contribution to EXAFS is also significant.

Transformation from crystalline to metamict zircon. The transformation into the metamict state results in two modifications of the EXAFS spectra: an important loss of medium range order and a coordination change around Zr in highly damaged zircons. The less metamict samples ($\mathscr{R}$ down to 0.07) show the interatomic distances characteristic of the zircon structure, although with some disorder on the second and more distant atomic shells. A dramatic loss of intensity is evidenced in the FT for $\mathscr{R}$ values between 0.07 and 0.05 and the contribution of the shells beyond the first are almost nonexistent (Fig. 1). At $\mathscr{R}$ values lower than 0.05, EXAFS oscillations approximate a single damped sine function and are no longer detected at $k > 12$ Å^{-1}. At this stage, the first coordination shell largely prevails and only a second weak contri-

TABLE 5. Table of crystalline compounds used for Th data reduction

Compound	EXAFS results	Structure refinement data	References
Th-O*			
Thorite (α-$ThSiO_4$; synthetic)	8.0 × O at 2.41 Å (0.06)	8 × O at 2.405 Å (0.06)	Taylor and Ewing, 1978
Huttonite (β-$ThSiO_4$; synthetic)	8.9 × O at 2.47 Å (0.10)	9 × O at 2.50 Å (0.13)	Taylor and Ewing, 1978
Th-nitrate (pentahydrate, synthetic)	10.8 × O at 2.51 Å (0.07)	11 × O at 2.54 Å (0.06)	Ueki et al., 1966 Taylor et al., 1966
Uncertainties estimated for Th-O: ±0.5 for CN; ±0.02 Å for R and σ			
Th-Si**			
Thorite	2.0 × Si at 3.17 Å (0.03)	2 × Si at 3.16 Å (0.00)	Taylor and Ewing, 1978
	4.0 × Si at 3.92 Å (0.02)	4 × Si at 3.90 Å (0.00)	Taylor and Ewing, 1978
Uncertainties estimated for Th-Si: ±1.0 for CN; ±0.02 Å for R and σ			

* ThO_2 data: 8 × O at 2.405 Å; σ = 0.000 (Wyckoff, 1963).
** McKale data (McKale et al., 1988).

bution is observed (Fig. 1). EXAFS-derived Zr-O distances decrease from 2.20 Å to 2.13 Å with increasing metamictization and are consistent with sevenfold coordination (Table 7). Disorder effects are responsible for the increase of $\Delta\sigma/BaZrO_3$ from 0.06 to 0.10 Å with decreasing $\mathcal{R}$. The weak contributions at larger interatomic distances arise from Si- and Zr-atomic shells. They are responsible for the interferences observed near 8–10 $Å^{-1}$ in the inverse FT (Fig. 2). The intensity of the Zr-Zr contribution decreases with increasing metamictization down to below the detection limit in totally metamict zircons. When measurable, Zr-Zr distances are found at a constant value of 3.34 Å and are shorter than in crystalline zircon (3.64 Å) and in baddeleyite (3.47 Å ± 0.07). The Zr-Si distance remains constant at 2.9–3 Å. In both cases, the weak intensity of the Zr-Zr and Zr-Si contributions results from disorder effects, which hinder determination of actual coordination numbers. The difference of the FT modulus between that of metamict zircon and that of baddeleyite excludes any decomposition into crystalline oxide components during metamictization.

Spectroscopic results on minor components in Näegi no. 2 zircon

As in the case of Zr-EXAFS, Th- and U-L_{III} EXAFS spectra are strongly attenuated for k values greater than 9 $Å^{-1}$, which excludes any clustering of crystalline phases containing these elements. Because simple oxides (e.g., thorianite, uraninite) can sustain important radiation doses without damage, they do not occur in the metamict state (Ewing et al., 1987) and would thus be detected by EXAFS. Hf-O distances (Table 8) at 2.25 Å and the apparent coordination number together with a $\Delta\sigma$ value of 0.04 Å all suggest eightfold coordinated Hf. These data suggest a regular substitution of Zr in the zircon structure. Th is also in eightfold coordination with mean Th-O distances of 2.41 Å and $\Delta\sigma/ThO_2$ = 0.08 Å (Table 8). Optical absorption spectra (Fig. 3) indicate that U(IV) is primarily present in this sample, without any significant contribution from higher oxidation states. A similar optical absorption spectrum is found in reduced U(IV)-bearing diopside glass (see Calas, 1979) and in metamict zircon from Sri Lanka. Weak U(V) absorption bands are found near 7000 cm^{-1} and have been mentioned as occurring in Sri Lanka zircon (Vance and Mackey, 1974). U-L_{III} EXAFS arises only from the first O coordination shell at a significantly smaller distance compared to UO_2 (Fig. 4). Short U(IV)-O distances (as compared to UO_2) are calculated to be at 2.28 Å (Table 8), associated with $\Delta\sigma$ = 0.05 relative to UO_2 and a coordination number of about 6.

Local structure around Th in metamict thorium silicates

The FT of Th-L_{III} EXAFS of synthetic thorite (Fig. 5) reflects the local structure predicted from structure refinements (Taylor and Ewing, 1978). The contribution of the nearest Si-shell is better resolved on the FT in thorite than in zircon owing to the different next-nearest neighbors (and thus different backscattering phase-shift functions). The disappearance of medium range order is the most salient feature observed during thorite metamictiza-

TABLE 6. Table of crystalline compounds used for U data reduction

Compound	EXAFS results	Structure refinement data	References
Axial U-O distances [U-O < 2 Å]*			
Cuprosklodowskite (Musonoï, Zaïre)	1.8 × O at 1.79 Å (0.00)	2 × O at 1.77 Å (0.00)	Rosenzweig and Ryan, 1975
Uranyl sodium nitrate (synthetic)	2.0 × O at 1.76 Å (0.00)	2 × O at 1.76 Å (0.01)	Taylor and Mueller (1969)
Uncertainties estimated for U-O_{axial}: ±0.5 for CN; ±0.02 Å for R and σ			
Other U-O distances [U-O > 2 Å]**			
Cuprosklodowskite (Musonoï, Zaïre)	5.2 × O at 3.34 Å (0.07)	5 × O at 2.36 Å (0.06)	Rosenzweig and Ryan, 1975
Uranyl sodium nitrate (synthetic)	6.2 × O at 2.42 Å (0.02)	6 × O at 2.42 Å (0.00)	Taylor and Mueller (1969)
Uncertainties estimated for U-$O_{equatorial}$: ±0.5 for CN; ±0.02 Å for R and σ			

* Uranyl sodium acetate data: 2 × O at 1.76 Å; σ = 0.00 (Templeton et al., 1985).
** UO_2 data: 8 × O at 2.385 Å; σ = 0.000 (Wyckoff, 1963).

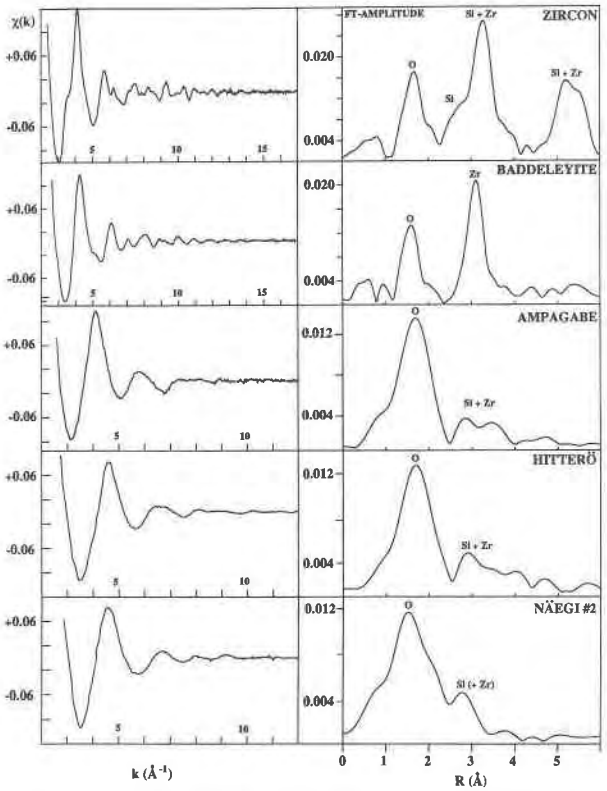

Fig. 1. Moduli of the Fourier transforms of selected zircon samples at the Zr-*K* edge compared to that of baddeleyite. Peaks are indexed during data reduction and their positions are uncorrected for backscattering phase shifts. See text for detailed explanations.

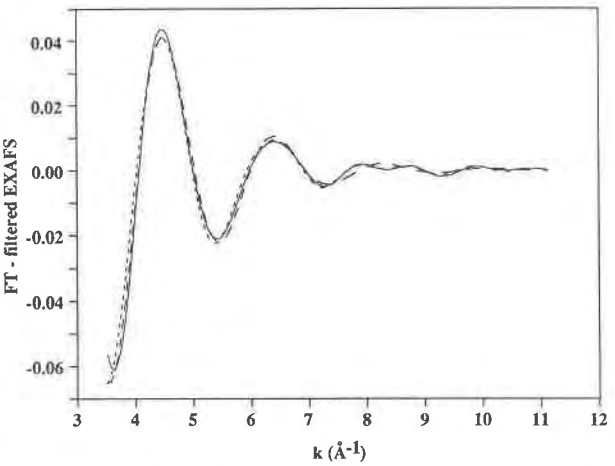

Fig. 2. Example of data reduction at the Zr-*K* edge in metamict zircon from Hitterö (Norway). Solid line: experimental Fourier filtered spectrum; dashed line: calculated spectrum with O atoms at 2.13 Å; dotted line: calculated spectrum involving O atoms at 2.13 Å + Si atoms at 2.86 Å and Zr atoms at 3.34 Å. Interferences near 8.3 and 10.4 $Å^{-1}$ are essentially generated by Zr atoms.

tion and only nearest neighbors contribute to EXAFS (Fig. 5). In metamict thorite Th-O interatomic distances and Th-coordination numbers remain at the same value as in crystalline thorite (Table 9). A significant increase of the $\Delta\sigma/ThO_2$ factor is observed with increasing alpha-event dose. A weak contribution of the next nearest neighbors (Si) is observed at the EXAFS detection limit.

EXAFS spectra of the two thorogummite samples are similar to that of metamict thorite. No medium range order is detected around the ThO_8 polyhedra. The major difference concerns the reduction of the $\Delta\sigma/ThO_2$ parameter to values lower than in crystalline thorite. The $\Delta\sigma/ThO_2$ value goes down to zero in the Iazaka thorogummite as in thorianite. A contribution from next-nearest neighbors (Si) is detected but is too weak to be modeled.

Local structure around U in metamict thorium silicates

The samples investigated show a wide range in U content (between 4.16 and 14.91 wt% UO_2). On account of their yellow to brown color ("orangite" variety), all thorite samples were investigated with optical absorption spectroscopy (Fig. 6). The yellow color of the uranothorite from Tvegestrand results from an intense absorption near 23000 cm^{-1}, characteristic of O → U charge transfer transitions in uranyl groups UO_2^{2+} (Calas, 1979). No 5f → 5f absorption bands are found indicating the absence of lower oxidation states. In orange samples the contribution of the ferric oxides hinders the observation of the

TABLE 7. Extracted structural parameters for metamict zircon at the Zr-*K* edge

	O			Si			Zr			E_0	ΔE	Correlation
	R (Å)	*N*	$\Delta\sigma$ (Å)	*R* (Å)	*N*	$\Delta\sigma$ (Å)	*R* (Å)	*N*	σ (Å)	(eV)	(eV)	coefficient
Crystalline Australia	2.20	8.0	0.06	2.95	2.3	0.03	3.62	4.0	0.06	17994.1	+0.1	0.03933
Crystalline Brazil	2.19	8.0	0.06	2.95	1.8	0.03	3.64	3.4	0.06	17994.2	+0.1	0.04015
Metamict Miask	2.19	8.0	0.06		UM*		3.62	2.7	0.07	17944.2	+0.4	0.00743
Metamict Betafo	2.15	7.0	0.09	2.82	1.1	0.04	3.31	0.9	0.06	17994.1	−0.7	0.00943
Metamict Ampagabe	2.14	6.9	0.09	2.86	0.9	0.04	3.34	1.1	0.05	17994.0	−0.7	0.00940
Metamict Hitterö	2.13	7.1	0.10	2.86	0.6	0.02	3.34	0.5	0.04	17992.6	+0.8	0.00187
Metamict Näegi no. 1	2.13	6.8	0.10	2.90	0.4	0.00	3.34	0.9	0.07	17991.4	+0.4	0.00243
Metamict Näegi no. 2	2.13	7.1	0.10	2.88	0.9	0.00		UM*		17991.2	+0.0	0.00475
Metamict Kinkle's Quarry	2.13	7.2	0.10	2.86	0.5	0.00		UM*		17995.0	−1.1	0.00111

* Contribution detected but not included in model.

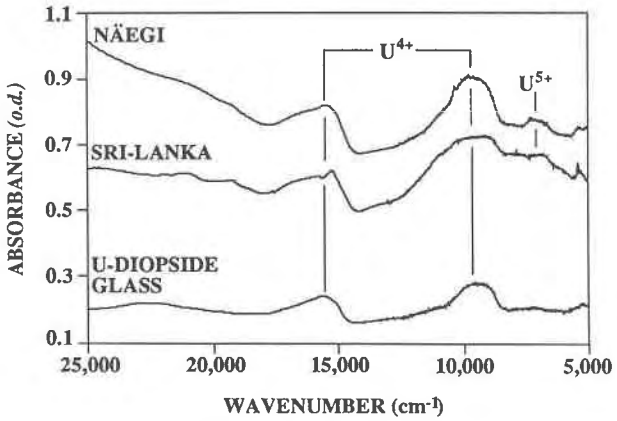

Fig. 3. Diffuse reflectance optical absorption spectrum of selected metamict zircon samples. From top to bottom: zircon Näegi no. 2 (color: dark green), zircon from Sri Lanka (0.5 × 10^{16} α/mg: light green), 3 wt% U(IV)-containing CaO-MgO-2SiO_2 glass (diopside composition) synthesized at $f_{O_2} = 10^{-9.5}$ atm and at 1450 °C (Laboratory of Experimental Petrology, University of Edinburgh; color is green). Peaks in the spectra arise from U(IV) absorption but a weak but significant contribution from U(V) is detected in the highly damaged zircon Näegi no. 2.

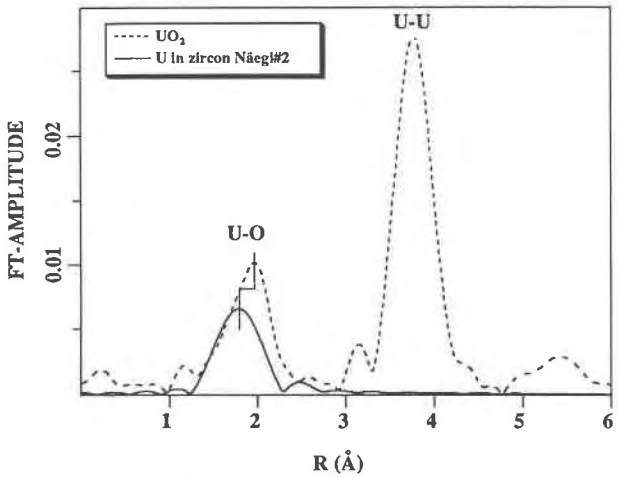

Fig. 4. U-L_{III} edge FT in zircon Näegi no. 2 (plain line) compared to UO_2 (dashed line) where U(IV) is eightfold coordinated. The figure shows an enlarged view of the O peak, truncating the intense U-U contribution of UO_2. Peak positions are in ångströms and uncorrected for phase shifts.

absorption bands from uranyl groups. U-L_{III} XANES (Fig. 7) is similar to that observed in uranyl compounds (cuprosklodowskite, uranyl nitrate and uranyl-sodium acetate). A chemical shift of 8 eV toward higher energy compared to UO_2 implies that U is hexavalent. The localization of 5f electrons has been recently studied in a variety of U-compounds (Petiau et al., 1987; Petit-Maire, 1988) and the uranyl groups are clearly identified by a resonance located on the high energy side of the absorption edge about 5–8 eV above the edge crest (Fig. 7). XANES and optical spectroscopy thus clearly indicate that most U (more than 90%) occurs as uranyl groups in the thorium silicates investigated in this study. U-L_{III} EXAFS spectra have been measured in thorite and uranothorite and are significantly reduced for $k > 12$ Å^{-1}. The FT shows an asymmetric peak due to O nearest neighbors with no other significant contributions. The U-O distances (Table 8) show two groups of O atoms, interpreted as the axial and equatorial groups which constitute the uranyl complexes.

Discussion

Evolution of local order during metamictization

Disorder effects. Disorder effects must first be considered because they could be responsible for an apparent decrease in the interatomic distances and coordination numbers as already observed in transition element-bearing silicate glasses (Calas and Petiau, 1983). Non-Gaussian distance-distribution models (de Crescenzi et al., 1981) applied to our analyses were found to give similar interatomic distances as compared to a harmonic (i.e., Gaussian) model. First and further atomic shells will be separately discussed, as short range and medium range order are not directly related (Gaskell, 1985; Cheng and Johnson, 1987). Both site distributions and variations of interpolyhedral relations will contribute simultaneously to radial disorder effects, and it is difficult to separate these effects.

First coordination shell. The first step of metamictization ($\mathscr{R} \geq 0.07$) does not show any significant modification of the O polyhedron (Fig. 8). In the second step ($\mathscr{R}$ ranging from 0.07 to 0.03), Zr-O distances and Zr coordination number decreases with metamictization. At $\mathscr{R} = 0.03$, Zr is sevenfold coordinated with Zr-O distances of 2.15 Å. The third step ($\mathscr{R}$ lower than 0.03) corresponds to almost totally metamict zircons. The average Zr-O distance decreases slightly to 2.13 Å with decreasing $\mathscr{R}$ and constant σ. No differences are observed in the measured Zr coordination number which remains

Table 8. Extracted structural parameters for minor elements in metamict zircon and thorite

	O			E_0	ΔE	Correlation
	R (Å)	N	$\Delta\sigma$ (Å)	(eV)	(eV)	coefficient
Metamict zircon Näegi no. 2						
Hf-L_{III} edge	2.25	7.0	0.04			
U-L_{III} edge	2.28	5.5	0.05	17152.1	+0.1	0.00251
Th-L_{III} edge	2.41	8.0	0.08	16281.6	+0.1	0.00910
Annealed zircon Näegi no. 2*						
Th-L_{III} edge	2.41	8.0	0.03	16283.8	−0.1	0.00223
U-L_{III} edge in uranothorites**						
Arendal						
Axial O	1.81	2.0	0.00	17158.8	−0.8	0.00244
Equatorial O	2.32	4.2	0.09			
Tvegestrand						
Axial O	1.78	2.2	0.04	17159.1	−1.0	0.01280
Equatorial O	2.20	4.5	0.15			

* Annealing conditions: in air at 1300 °C during 15 h.
** U(VI)O_2^{2+} (uranyl) group in all samples.

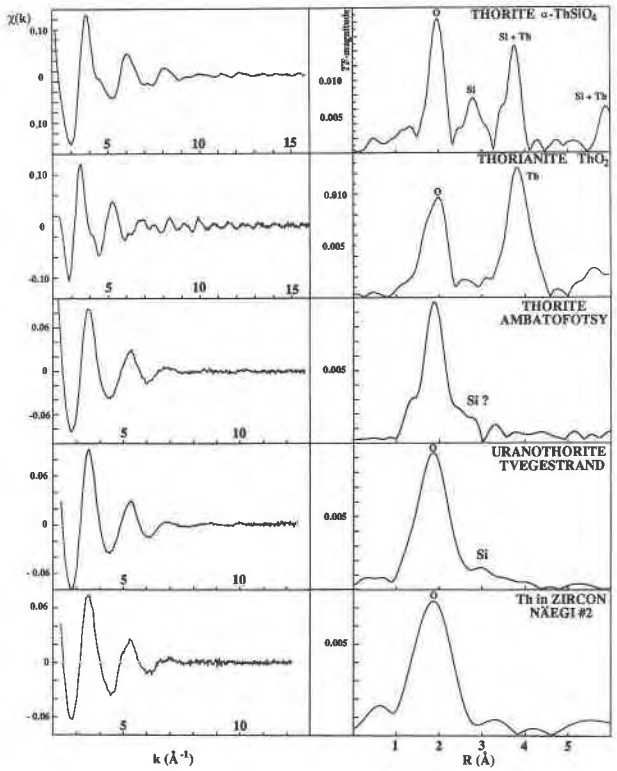

Fig. 5. Moduli of the Fourier transforms of selected thorium metamict silicates at Th-L_{III} edge compared to that of thorianite. Peaks are indexed during data reduction and are uncorrected for phase shifts.

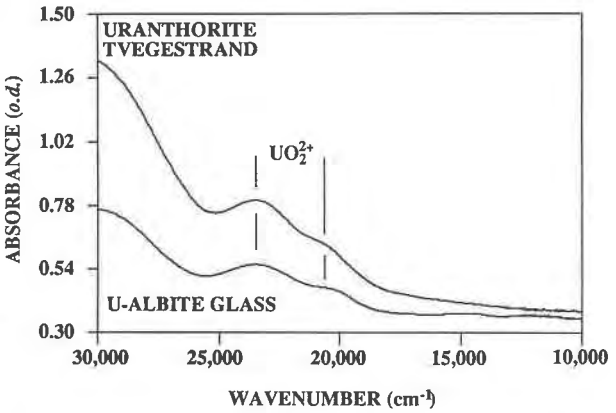

Fig. 6. Diffuse reflectance optical absorption spectrum of uranothorite from Tgevestrand (top) compared to glass containing 1 wt% U(VI) and of composition (Na_2O-Al_2O_3-$6SiO_2$) (albite composition) synthesized in air and at 1250 °C. Both show the absorption peaks characteristic of the uranyl group $U(VI)O_2^{2+}$. No other contribution [including U(V) and U(IV)] was detected in this thorite spectrum.

at approximately 7. Hence, extensive site mixing is excluded on account of the nearly constant coordination of Zr(7).

In metamict zircon, the mean Zr-O distance is characteristic of the sevenfold coordination (baddeleyite: 2.17 Å). Relict crystalline domains have been detected even at high levels of radiation damage by XRD (Murakami et al., 1986; Vance et al., 1980; Özkan, 1976), HRTEM (Yada et al., 1981; Headley et al., 1981; Yada et al., 1987; Chakoumakos et al., 1987), and positron annihilation studies (Vance et al., 1980). Such domains are not detected by EXAFS and are probably of minor importance (less than 10% of Zr atoms). These results disagree with recent X-ray scattering analyses which concluded that there were similar Zr-O distances in Naëgi metamict and crystalline zircon samples (Sugiyama and Waseda, 1989). A possible explanation lies in the metamictization state, because only totally metamict zircons (as Näegi no. 2) exhibit unique structural properties. Another limitation comes from the absence of chemical selectivity of X-ray scattering techniques. A decrease of the Zr-O distances between crystalline and metamict zircon has been ascribed to the presence of impurities, based on a qualitative interpretation of EXAFS data (Nakai et al., 1987). With complete data reduction, this study demonstrates the absence of any influence of the impurity content on Zr-O distances (e.g., in samples from Näegi no. 1 and Hitterö). The coordination number of Th is 8 in crystalline and metamict

Table 9. Extracted structural parameters for metamict thorite, uranothorite, and thorogummite at Th-L_{III} edge

	O			Si			E_0	ΔE	Correlation
	R (Å)	N	$\Delta\sigma$ (Å)	R (Å)	N	$\Delta\sigma$ (Å)	(eV)	(eV)	coefficient
Thorite									
Ambatofotsy, Madagascar	2.42	7.8	0.07		UM*		16283.8	−0.1	0.00220
Unknown locality, Madagascar	2.41	7.8	0.09	3.20	0.7	0.00	16285.0	−0.9	0.00643
Andranomitroky, Madagascar	2.44	8.0	0.08		ND**		12284.6	−0.3	0.00677
Brevik, Norway	2.42	7.8	0.10		ND**		16284.4	−0.3	0.00165
Uranothorite									
Arendal, Norway	2.39	7.7	0.08	3.22	0.6	0.00	16281.2	−0.1	0.00379
Svenes, Norway	2.43	7.7	0.09		UM*		16282.0	0.0	0.00419
Tvegestrand, Norway	2.43	7.7	0.10	3.22	0.6	0.00	16284.0	+0.1	0.01473
Thorogummite									
Iazaka, Japan	2.39	7.8	0.00		UM*		16285.0	−0.8	0.01603
Andranomitroky, Madagascar	2.41	8.0	0.05		ND**		16282.8	0.0	0.00499

* Not included in model.
** Not detected.

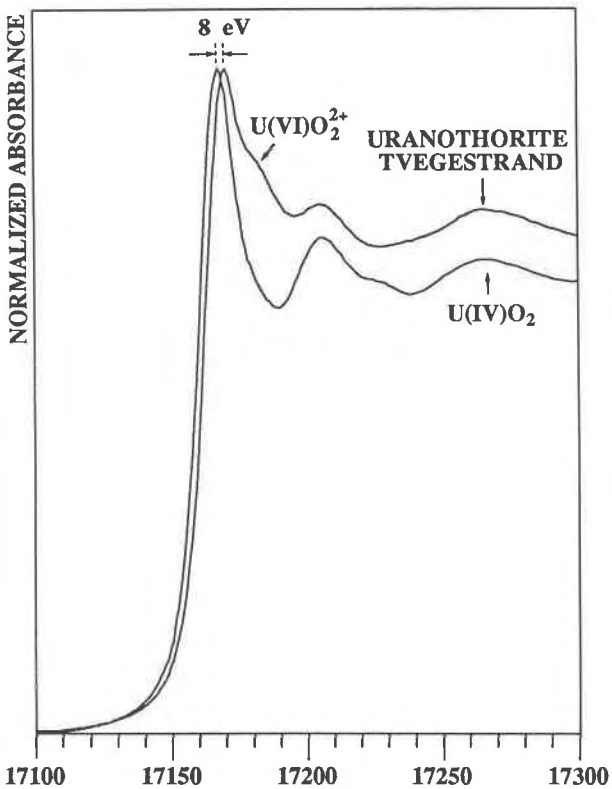

Fig. 7. XANES spectrum of uranothorite from Tvegestrand compared to uraninite at the U-L_{III} edge. The edge of the XANES spectrum of metamict thorite is shifted to higher values of energy compared to that of uraninite [U(IV)]. This is characteristic of the presence of U(VI). The asymmetric signal of the edge is characteristic of the uranyl group U(VI)O$_2^{2+}$. Abscissa units are energy (eV).

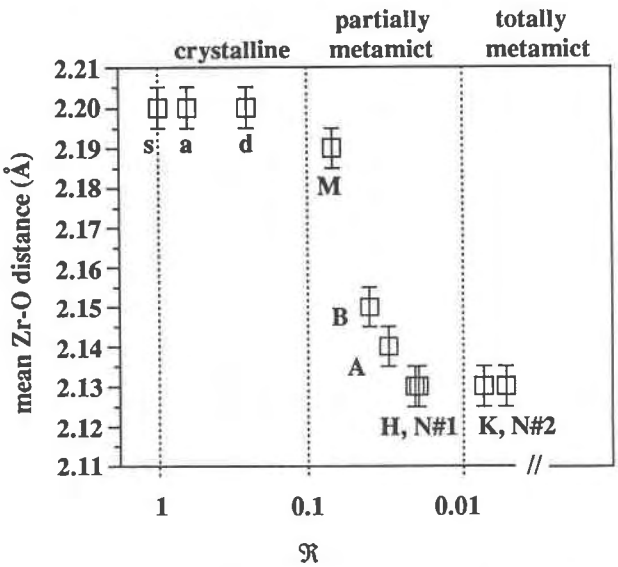

Fig. 8. Evolution of the mean Zr-O distance (Å) with increasing radiation damage (ratio $\mathscr{R}$). Letters refer to samples: lower case letters = crystalline samples: s = synthetic; a = Alice Springs, Australia; d = Diamantina, Brazil. Capital letters = partially and totally metamict zircons: M = Miask, U.S.S.R.; B = Betafo, Madagascar; A = Ampagabe, Madagascar; H = Hitterö, Norway; N#1 = Näegi no. 1; N#2 = Näegi no. 2, Japan; K = Kinkle's Quarry, Bedford, U.S.A. The error bars are estimated on the basis of data for reference compounds.

thorite, and the only modifications are in the relative $\Delta\sigma/ThO_2$ factor which increases with metamictization from 0.06 to 0.10 Å.

EXAFS thus detects differences in Zr and Th in metamict silicates. This can be due to a difference in alpha-dose or crystal chemistry. The possibility of finding both elements in the same sample (Näegi no. 2 zircon) points out the importance of the second factor. Of great importance is that the effective ionic radii are different: 0.84 Å and 1.05 Å for eightfold coordinated Zr(IV) and Th(IV), respectively (Shannon and Prewitt, 1976). The average coordination number of Zr coordinated by O or F is 6.7 at ordinary pressures and the coordination number predicted using ionic radius ratios is 7 (Brown, 1988). Metamictization would thus be described as a relaxation of the ZrO_8 polyhedron of zircon to a more stable local configuration. In contrast, Th-bearing minerals primarily contain eightfold coordinated Th, with the exception of phases with the monazite structure (brabantite, huttonite) with ninefold coordination. Octahedral Th is still unknown in minerals. Structure refinements are needed to define the coordination of Th in sodium thorium silicates (mostly metamict) found in alkaline rocks, such as thornasite (Ansell and Chao, 1987) and umbozerite (Es'kova et al., 1974). Such behavior may account for similar Th-O distances in crystalline and metamict thorites.

The further atomic shells

The presence of Zr-Si atomic pairs with interatomic distances around 2.9–3 Å corresponds to edge-sharing SiO_4 and ZrO_n polyhedra, as in crystalline zircon. This kind of contribution apparently decreases with decreasing $\mathscr{R}$. The change of the average coordination number of Zr from 8 to 7 will tend to result in smaller Zr-Si distances corresponding to edge-sharing polyhedra, owing to the decrease of both Zr-O distances and Zr-O-Si angles. As significant disorder is observed on the Si-shell, some structural reorganization of the SiO_4 tetrahedra among themselves is possible, corresponding to the features attributed to amorphous silica in infrared spectra (Vance, 1975). Th-Si distances show less variation in metamict thorite than Zr-Si distances in metamict zircon. This is consistent with the constant Th-O distance observed during thorite metamictization.

The contribution of Zr-Zr pairs to EXAFS regularly decreases with $\mathscr{R}$ but the low intensity makes its analysis difficult in totally metamict zircon (Kinkle, Näegi). The smaller Zr-Zr distances (3.34 Å instead of 3.64 Å) correspond to edge-sharing ZrO_7 polyhedra, as in baddeleyite, but at a slightly smaller distance. This is consistent

with conclusions drawn from Zr-Si contributions. Edge-sharing ZrO_n-ZrO_n and ZrO_n-SiO_4 polyhedra exist at all stages of metamictization, with n decreasing from 8 to 7 with decreasing $\mathscr{R}$.

A model for metamictization

In the absence of information concerning the behavior of silicate groups during metamictization, it is not possible to draw a complete picture of the structural transformations which occur during alpha-decay damage of zircon and thorite. The major change observed in this study corresponds to a coordination change around Zr and not around Th, probably due to differences in ionic radii. The possibility that Zr adapts to a lower coordination number is important in a process which is largely dominated by the creation of O vacancies (Vance et al., 1980). If O atoms remain bonded in SiO_4 tetrahedra during alpha-collision and recoil-nuclei radiation damage, the creation of O vacancies may thus be understood as a displacement or tilting of the SiO_4 tetrahedra. This mechanism results in a decrease of the coordination number of Zr. The creation of further O vacancies will lead concurrently to a progressive polymerization of silicate tetrahedra, a process which has only been indirectly supported by infrared spectroscopy (Vance, 1975). When the possibility that an atom has a lower coordination number is constrained as in Th, the topological relations with the surrounding polyhedra cannot be maintained and the initial local structure in the 3–4 Å range is destroyed. This is indeed observed in thorite and in Th-bearing zircon, in which no ThO_8-ThO_8 edge-shared linkages are detected with EXAFS.

The structure of metamict silicates corresponds to defects in an ordered structure, in which the disordered state is defined in terms of defects in the ordered state (Gaskell, 1985). In this model, strict topological constraints influence the relations between the constituent polyhedra, in contrast to observations of silicate glasses (see below). The local topology is favored by the stable coordination of the cation, which is predicted to be 7 and 8 for Zr and Th, respectively (Brown, 1988). The failure to reach an ordered structure results from kinetic constraints, as shown by annealing experiments of metamict zircon and thorite which allow recovery of crystallinity.

The role of H-O species in metamictization also must be taken into account. Molecular H_2O (Mumpton and Roy, 1961), hydroxyl groups (Caruba et al., 1985), or H-O species (Aines and Rossman, 1985, 1986) may stabilize the metamict state in zircon. As evidenced by the chemical analyses presented in this paper, there is no clear relation between the content of H-O species and degree of metamictization. No direct information can be derived from EXAFS spectra concerning the presence of OH groups bound to Zr or Th, as O- and OH-contributions cannot be separated with EXAFS. The stabilizing role of hydroxyl groups can arise from bond breaking (silanol and ZrOH groups) and from the relaxation of structural constraints imposed by the stoichiometry. The Zr-OH and Si-OH groups give smaller Zr-Zr and Zr-Si contributions to EXAFS, respectively, as is also true for thorite.

Other structural relations

The steps recognized in the evolution of EXAFS parameters during zircon metamictization may be compared to the stages already described on the basis of XRD, microstructures, or optical properties (Holland and Gottfried, 1955; Murakami et al., 1986). The first stage of metamictization ($\mathscr{R} \geq 0.2$) corresponds to a large increase of the a-cell parameter from 6.604 to 6.67 (Table 1), although no significant changes are observed in the local structure around Zr. The radiation damage primarily causes the displacement of O atoms, with resultant small radial disorder (Vance et al., 1980). If SiO_4 tetrahedra are assumed to be nonpolymerized at this stage, as indicated from infrared spectra, this implies a less efficient packing of the atoms and a corresponding expansion of the cell volume. The expansion coefficient for c is greater than for a. In crystalline zircon, **c** and **a** correspond to edge-shared ZrO_8-SiO_4 and ZrO_8-ZrO_8 polyhedra, respectively. A larger expansion coefficient is consistent with Si-O bonds being stronger than Zr-O bonds, as well as with the presence of rigid SiO_4 tetrahedra.

The second stage ($\mathscr{R}$ from 0.2 to 0.07) shows relict zircon domains (with sightly larger cell parameters) coexisting with aperiodic domains (Murakami et al., 1986; Yada et al., 1981). Because EXAFS gives an average picture of this material, the more abundant amorphous phase gives the major contribution. This could account for the apparent discrepancy between XRD and EXAFS; i.e., the c parameter increases slightly whereas Zr-O distances decrease. Whereas EXAFS gives access to the average environment around Zr, XRD is sensitive primarily to the evolution of the relict zircon crystalline domains. The defect-containing ordered model presented above explains why the diffuse scattering arising from the amorphous regions remains near the positions of the Bragg reflections of ziron (Vance et al., 1980).

The third stage ($\mathscr{R} < 0.02$) cannot be characterized by diffraction methods, but density still decreases at high alpha-decay doses (Ewing et al., 1987). Effects of disorder strongly limit the accuracy of EXAFS as this method can not detect further structural changes. Effects of disorder affect the long range order more than the nearest neighbors, as observed in the progressive loss of Zr-Zr contributions in the most highly metamict zircon. A stable local structure is also reached in thorite.

Comparison with Zr-, Th-, and U-bearing silicate glasses

The O polyhedra around Zr in metamict zircon are very different than those observed in glasses in which Zr is in sixfold coordination (Brown and Ponader, 1986; Farges and Calas, 1987, in preparation). Si atoms are observed with a Zr-Si distance of 3.64–3.69 Å (corner-sharing polyhedra), and no Zr-Zr contribution to EXAFS is

found. The local structures of metamict and vitreous Zr-bearing silicates are thus very different, in contrast to the assumptions of Nakai et al. (1987). Similarly, Th is essentially sixfold coordinated in silicate glasses, with some contribution from higher coordination numbers (Farges and Calas, 1988). This unusual coordination number is also at variance with the local structure found in Th-bearing metamict silicates. Only U(IV) is found in both silicate glasses and metamict zircon in a distorted octahedral environment.

The Zr-O distance regularly decreases in metamict zircon to 2.13 Å in the most damaged sample. This distance is close to the value at which sevenfold coordination may become unstable in favor of a sixfold coordination (≈2.11 Å). This suggests that only an unusually high radiation dose (perhaps not yet encountered in natural zircon) may lead to sixfold coordinated polyhedra around Zr. This would imply the creation of a second O vacancy per ZrO_n polyhedron. No such samples have been found, probably due to the absence of such severe radiation conditions.

The behavior of actinides in metamict zircon and thorite

Substitution of actinides in zircon occur only if accompanied by large structural relaxation processes, because of the differences in ionic radii (Speer and Cooper, 1982). Their behavior may be obscured by crystal zoning (Chakoumakos et al., 1987; Schärer and Allègre, 1982; this study) or the presence of very small inclusions (i.e., not detected at the microprobe scale). Special attention has been paid to the Näegi no. 2 metamict zircon because of its high concentration of minor components (Table 2). The local structure around Th is near that observed in metamict thorite, and no Th-Zr pairs have been detected. Because of the eightfold coordination of Th, metamict thorite is the only likely alternative to an ideal substitution process. Indeed, as no Th-Th pairs are seen in the annealed sample (1300 °C/15 h) the presence of significant thorite domains is excluded.

EXAFS data for U(IV) in metamict zircon indicate an original, sixfold coordination for U(IV). A qualitative comparison of optical absorption spectra indicates the same environment in zircon from the Urals and Sri Lanka. The absence of any U-U contribution to EXAFS in both metamict and annealed zircon suggests the absence of U-bearing phases, although the substitution of U for Zr cannot be proven in the absence of U-Zr contributions, as in the case of Th.

Uranothorite contains U mostly as uranyl groups (usually 2 axial O atoms at 1.78–1.81 Å and 4–5 equatorial O atoms at 2.2–2.3 Å). No medium-range order is detected, so that uranyl groups may be incorporated in amorphous domains rather than in uranyl containing very small inclusions. Oxidation processes are subsequent to the formation of phases belonging to the $USiO_4$-$ThSiO_4$ solid solution series (tetravalent actinides) and probably occur during metamictization to give secondary uranyl groups UO_2^{2+}. Because the uranyl groups can be easily leached, the alpha-dose values given in Table 1 are underestimated. Metamict thorite coexists with partly metamict zircon, as in Norwegian samples. U is tetravalent in such zircon whereas uranyl groups are detected in the thorite. Both minerals show a well-defined sensitivity to weathering processes, because of the differences in the alpha event-dose. Finally, thorogummite results from surficial weathering which tends to produce a short-range local environment around Th similar to that of thorianite. Decomposition into simple oxides may explain thorogummite formation because weathering is significantly enhanced by radiation damage in most metamict minerals, including zircon (Ewing et al., 1987; Petit et al., 1985; Krogh and Davis, 1975).

Conclusions

The XAS data presented in this paper on metamict silicates define the immediate environment of Zr and Th during metamictization. In contrast to XRD, the data are obtained from all material, not just from the crystalline relict domains. Some results illustrate the consistency of the behavior of most elements during metamictization of complex oxides; i.e., the reduction of the coordination numbers and cation-O distances around Zr. The stoichiometry of the simple silicates $MeSiO_4$ requires additional constraints on the possible local changes. Metamictization is accompanied by a loss of medium range order and significant apparent modification of the second coordination sphere; this change depends on the modification of the first coordination shell. If the cation can take a lower coordination number (as in the case of Zr), a coordination change allows the local structure to be partially maintained during metamictization. If not, as for Th, the local structure is rapidly destroyed.

However, in the case of metamict silicates, the SiO_4 groups play a specific role because of their rigidity and their ability to polymerize as a response to the creation of the O vacancies induced by radiation. More data are needed for a complete picture of the metamict state through a description of the behavior of silicate groups during metamictization. Some infrared data have strongly suggested the presence of amorphous silica domains which would give a nonrandom aperiodic model in contrast to observations in most complex metamict oxides. There is also a strong difference in the local structure around Zr and Th in silicate glasses, which reflects the diversity of local structures encountered in amorphous silicates.

Acknowledgments

François Farges is indebted to the Société de Secours des Amis des Sciences (Paris) for financial support. We are also indebted to P. Bariand, J.F. Poullen, H.J. Schubnel, M. Skrok, F. Cesbron, M.P. Lahalle, P. Berthet, and B. Mottet for providing the samples used in this study. We thank H. Vachey for Penfield gravimetric analyses, H. Remy for technical assistance with electron microprobe analyses, and D. Petit-Maire and the staff of LURE for their assistance during data acquisition and reduction. This manuscript was greatly improved by comments of G.E. Brown, Jr.

and E. Fritsch and the critical reviews of R.C. Ewing, G. Rossman, and G.A. Waychunas. This work was supported by the CNRS/INSU. Contribution CNRS/INSU/DBT-24/Thème Fluides-Cinétiques.

References cited

Aines, R.D., and Rossman, G.R. (1985) The high temperature behavior of trace hydrous components in silicate minerals. American Mineralogist, 70, 1169–1179.

——— (1986) Relationships between radiation damage and trace water in zircon, quartz and topaz. American Mineralogist, 71, 1186–1193.

Alvi, M. (1976) Geology of the Bedford complex and surrounding rocks, southeastern New York (abs.). Dissertation Abstract International, 37, 123B.

Ansell, V.E., and Chao, G.Y. (1987) Thornasite, a new hydrous sodium thorium silicate from Mont Saint-Hilaire, Quebec. Canadian Mineralogist, 25, 181–183.

Barinsky, R.L., and Kulikova, I.M. (1977) Metamict transformations in some niobates and zircons according to X-ray absorption spectra. Physics and Chemistry of Minerals, 1, 325–333.

Besairie, H. (1970) Description géologique du Massif Ancien de Madagascar. Documentation du Service géologique, N° 177 a–d (4 vol.) 339 p. Ministère des Mines et de l'Energie, Direction des Mines et de l'Energie, Tananarive (in French).

Brown, G.E. Jr, and Ponader, C. W. (1986) X-ray absorption study of zirconium in Na-Zr-silicate glasses (abs.). International Mineralogical Association Abstracts with Programs, 63.

Brown, G.E., Jr, Calas, G., Waychunas, G.A., and Petiau, J. (1988) X-ray absorption spectroscopy: Applications in mineraology and geochemistry. The American Mineralogical Society Review in Mineralogy, 18, 431–512.

Brown, I.D. (1988) What factors determine cation coordination numbers? Acta Crystallographica, B44, 545–553.

Calas, G. (1979) Etude expérimentale du comportement de l'uranium dans les magmas: États d'oxydation et coordinance. Geochimica et Cosmochimica Acta, 43, 1521–1531 (in French).

Calas, G., and Petiau, J. (1983) Structure of oxide glasses. Spectroscopic studies of local order and crystallochemistry. Geochemical implications. Bulletin de Minéralogie, 106, 33–55.

Calas, G., Brown, G.E., Jr, Waychunas, G.A., and Petiau, J. (1987) X-ray absorption spectroscopic studies of silicate glasses and minerals. Physics and Chemistry of Minerals, 15, 19–20.

Cannillo, E., Rossi, G., and Ungaretti, L. (1973) The crystal structure of elpidite. American Mineralogist, 58, 106–109.

Caruba, R., Baumer, A., Ganteaume, M., and Iacconi, P. (1985) An experimental study of hydroxyl groups and water in synthetic and natural zircons: A model of the metamict state. American Mineralogist, 70, 1224–1231.

Chakoumakos, B.B., Murakami, T., Lumpkin, G.R., and Ewing, R.C. (1987) Alpha-decay-induced fracturing in zircon: The transition from the crystalline to metamict state. Science, 236, 1493–1600.

Chase, A.B., and Osmer, J.A. (1966) Growth and preferential doping of zircon and thorite. Journal of the Electrochemical Society, 113(2), 198–199.

Cheng, Y.T., and Johnson, W.L. (1987) Disordered materials: A survey of amorphous solids. Science, 235, 997–1002.

Chernyshev, I.V., Kononova, V.A., Kramm, W., and Grauert, B. (1987) Isotopic geochronoloy of Ural alkaline rocks based on zircon uranium-lead data. Geokhimya, 87(3), 323–338 (in Russian).

Correia Neves, J.M., Lopes Numes, J.E., and Sahama, T.G. (1974) High hafnium members of the zircon-hafnon series from the granite pegmatites of Zambezia, Mozambique. Contributions to Mineralogy and Petrology, 48, 73–80.

De Crescenzi, M., Balzarotti, A., Comin, F., Incoccia, L., Mobilio, S., and Motta, N. (1981) EXAFS measurements on Fe-B metallic glasses: Asymmetry of radial distribution function. Solid Sate Communcations, 37, 921–923.

Eisenberger, P., and Brown, G.S. (1979) The study of disordered systems of EXAFS: Limitations. Solid Sate Communications, 29, 481–484.

Es'kova, E.M., Semenov, E.I., Khomyakov, A.P., Mer'kov, A.N., Lebedeva, S.I., and Dubakina L.S. (1974) Umbozerite, a new mineral. Doklady Akademii Nauk SSSR, 216, 169–174 (in Russian).

Ewing, R.C., Chakoumakos, B.C., Lumpkin, G.R., and Murakami, T. (1987) The metamict state. Material Research Society Bulletin, 12/5, 58–66.

Farges, F. (1989) Organisation locale autour de Zr, Th et U dans des silicates amorphes: Minéraux métamictes et verres silicatés, 162 p. Thesis, Université Paris 7 (in French with abs. in English).

Farges, F., and Calas, G. (1987) XAS study of Zr-environment in silicate glasses: Relations with Zr-enrichment in magmatic suites (abs.). Terra Cognita, 7(2–3), 415.

——— (1988) X-ray spectroscopic study of heavy elements (Zr, Mo Th and U) in silicate glasses (abs.). Eos, 69, 1482.

Field, D., Craig Smalley, P., Lamb, R.C., and Råheim, A. (1985) Geochemical evolution of the 1.6–1.5 Ga-old amphibolite-granulite facies terrain, Bamble sector, Norway: Dispelling the myth of Greenvillian high-grade reworking. In A.C. Tobi and J.L.R. Touret, eds., The Deep Proterozoïc Crust in the North Atlantic Provinces, a Nato ASI series C issue, vol. 158. Reidel, Boston.

Frondel, C. (1953) Hydroxyl substitution in thorite and zircon. American Mineralogist, 38, 1007–1018.

Fuchs, L.H., and Gebert, E. (1958) X-ray studies of synthetic coffinite, thorite and uranothorites. American Mineralogist, 43, 243–248.

Gaskell, P. H. (1985) The structure of amorphous solids—A perspective view. Journal de Physique, 46, C8-3–C8-20.

Greegor, R.B., Lytle, F.W., Ewing, R.C., and Haaker, R.F. (1984) Ti-site geometry in metamict, annealed and synthetic complex Ti-Nb-Ta oxides by X-ray absorption spectroscopy. Nuclear Instruments and Methods in Physical Research, B1, 587–594.

Greegor, R.B., Lytle, F.W., Chakoumakos, B.C., Lumpkin, G.R., and Ewing, R.C. (1985a) An investigation of metamict and annealed natural pyrochlores by X-ray absorption spectroscopy. Materials Research Society Symposum Proceedings, 44, 655–662.

——— (1985b) An investigation of uranium L-edges of metamict and annealed betafite. Materials Research Society Symposium Proceedings, 50, 387–392.

——— (1986) Structural investigations of metamict minerals using X-ray absorption spectroscopy (abs.) 14th general meeting of the International Mineralogical Association, Stanford, California.

Greegor, R.B., Lytle, F.W., Chakoumakos, B.C., Lumpkin, G.R., Ewing, R.C., Spiro, C.L., and Wong, J. (1987) An X-ray absorption spectroscopy investigation of the Ta site in alpha-recoil damaged natural pyrochlores. Material Research Society Symposium Research, 84, 645–658.

Harker, A.B., and Flintoff, J.F. (1985) Crystalline-phase formation in hot isostasic pressing of nuclear waste ceramics with high zirconia content. Journal of the American Ceramic Society, 68(3), 159.

Hautefeuille, P., and Perrey, A. (1888) Sur la synthèse du zircon. Comptes-Rendus de l'Académie des Sciences de Paris, 107, 1000–1001 (in French).

Hawthorne, F.C. (1988) Spectroscopic methods in mineralogy and geology. In Mineralogical Society of America Reviews in Mineralogy, 18, 1–698.

Hazen, R.M., and Finger, L.W. (1979) Crystal structure and compressibility of zircon at high pressure. American Mineralogist, 64, 157–161.

Headley, T.J., Ewing, R.C., and Haaker, R.F. (1981) Amorphous structure of metamict minerals observed by TEM. Nature, 293, 449–450.

Holland, H.D., and Gottfried, D. (1955) The effects of nuclear radiation on the structure of zircon. Acta Crystallographica, 8, 291–300.

Hubin, P., and Tarte, P. (1971) Application de la spectrométrie d'absorption infrarouge à l'étude de la recristallisation de thorites métamictes. Bulletin de la Société Française de Minéralogie-Cristallographie, 94 471–476 (in French).

——— (1974) Etude expérimentale et interprétation du spectre infra-rouge des silicates et des germanates. Application à des problèmes structuraux relatifs à l'état solide. Mémoires de l'Académie Royale de Belgique, Classe des Sciences, (coll. in 8°), 35, fascicule 4a (in French).

Iimori, I., and Hata, H. (1938) Japanese thorogummite and its parent mineral. Scientific Papers of the Institute of Physical and Chemical Research, 34, 447–454.

Illyushin, G.D., Voronlov, A.A., Illyukhin, V.V., Nevskii, N.N., and Be-

lov, N.V. (1981) Crystal structure of natural monoclinic catapleiite $Na_2ZrSi_3O_9$-$2H_2O$. Soviet Physics Doklady, 26/9, 807–810.

Krogh, T.E., and Davis, G.L. (1975) Alteration in zircons and differential dissolution of latered and metamict zircon. Carnegie Institution Washington Yearbook, Geophysical Laboratory, 74, 619–623.

Lacroix, A. (1921–1923) Minéralogie de Madagascar, 2050 p. Challamel, Paris (in French).

Lumpkin, G.R., and Chakoumakos, B.C. (1988) Chemistry and radiation effects of thorite-group minerals from the Harding pegmatite, Taos County, New Mexico. American Mineralogist, 73, 1405–1419.

Lumpkin, G.R., Ewing, R.C., Chakoumakos, B.C., Greegor, R.B., Lytle, F.W., Foltyn, E.M., Clinard, Jr., F.W., Boatner, L.A., and Abraham, M.M. (1986) Alpha-recoil damage in zirconolite ($CaZrTi_2O_7$). Journal of Material Reserach, 1(4), 564–576.

Mackey, D.J., Runciman, W.A., and Vance, E.R. (1975) Crystal-field calculations for energy levels of U^{4+} in $ZrSiO_4$. Physical Review B, 11(1), 211–218.

McKale, A.G., Veal, B.W., Paulikas, A.P., Chan, S.K., and Knapp, G.S. (1988) Improved ab initio calculations of ampltude and phase functions for extended X-ray absorption fine structure spectroscopy. Journal of the American Chemical Society, 110, 3763–3768.

Mumpton, F.A., and Roy, R. (1961) Hydrothermal stability studies of the zircon-thorite group. Geochimica et Cosmochimica Acta, 21, 217–238.

Murakami, T., Chakoumakos, B.C., and Ewing, R.C. (1986) X-ray powder diffraction analysis of alpha-event radiation damage in zircon ($ZrSiO_4$). In D.E. Clark, W.B. White, and J. Machiels, Eds., Nuclear waste management II, vol. 20, Advances in ceramics, p. 745–753. American Ceramic Society, Columbus, Ohio.

Nagashima, O., and Nagashima, K. (1960) Rare elements minerals from Japan. Japan Mineral Club Press, Kyoto, Japan, 243–260.

Nakai, I., Akimoto, J., Imafuku, M., Miyawaki, R., Sugitani, Y., and Koto, K. (1987) Characterization of the amorphous state in metamict silicates and niobates by EXAFS and XANES analyses. Physics and Chemistry of Minerals, 15, 113–124.

Özkan, N. (1976) Effects of nuclear radiation on the elastic moduli of zircon. Journal of Applied Physics, 47/11, 4772–4779.

Pabst, A. (1952) The metamict state. American Mineralogist 37, 137–157.

Petiau, J., Calas, G., Petit-Maire, D., Bianconi, A., Benfatto, M., and Marcelli, A. (1987) Delocalized versus localized unoccupied 5f states and the uranium site structure in uranium oxides and glasses probed by X-ray absorption near-edge structure. Physical Review B, 34(10), 7350–7361.

Petit, J.C., Langevin, Y., and Dran, J.-C. (1985) Radiation-enhanced release of uranium from accessory minerals in crystalline rocks. Geochimica et Cosmochimica Acta, 49, 871–876.

Petit-Maire, D. (1988) Structure locale autour d'actinides et d'éléments nucléants dans des verres borosilicatés d'intérêt nucléaire: Résultats de spectroscopie d'absorption des rayons X, 198 p. Thesis (unpublished), Université Paris 6 (in French).

Richman, I., Kisliuk, P., and Wong, E.Y. (1967) Absorption spectrum of U^{4+} in zircon ($ZrSiO_4$). Physical Review, 155(2), 262–267.

Robinson, S.C., and Abbey, S. (1957) Uranothorite from eastern Ontario. Canadian Mineralogist, 6, 1–15.

Rosenzweig, A., and Ryan, R.R. (1975) Refinement of the crystal structure of cuproklodowskite $Cu[(UO_2)_2SiO_3(OH)_2]$-$6H_2O$. American Mineralogist, 60, 448–458.

Schärer, U., and Allègre, C.J. (1982) Uranium-lead system in fragments of a single zircon grain. Nature, 295, 585–587.

Shannon, R.D., and Prewitt, C.T. (1976) Revised effective ionic radii and systematic studies of interatomic distancs. Acta Crystallographica, 32, 925–946.

Smith, D.K., and Newkirk, H.W. (1965) The crystal structure of baddeleyite (monoclinic ZrO_2) and its relations to the polymorphism of ZrO_2. Acta Crystallographica, 18, 983–991.

Speer, J.A. (1982) Actinide orthosilicates. In Mineralogical Society of America Reviews in Mineralogy, 5, 113–135.

Speer, J.A., and Cooper, B.J. (1982) Crystal structure of synthetic hafnon, $HfSiO_4$, comparison with zircon and the actinide orthosilicates. American Mineralogist, 67, 804–808.

Staatz, M.H., Adams, J.W., and Wahlberg, J.S. (1976) Brown, yellow, orange and greenish-black thorites from the Seerie pegmatite, Colorado. Journal of Research of the United States Geological Survey, 4, 575–582.

Sugiyama, K., and Waseda, Y. (1989) Structural study of the metamict states by X-ray diffraction: In the case of naegite. Mineralogical Journal, 14, 303–309.

Takabatake, A. (1962) The Mino upper Cretaceous Sn-W province. In M. Saito, K. Hashimoto, H. Sawata, and Y. Shimazaki, Eds., Geology and resources of Japan (2nd edition), p. 143–170. Geological Survey of Japan, Tokyo.

Taylor, M., and Ewing, R.C. (1978) The crystal structure of $ThSiO_4$ polymorphs: Huttonite and thorite. Acta Crystallographica, B34, 1074–1079.

Taylor, J.C., and Mueller, M.H. (1969) A neutron diffraction study of uranyle nitrate hexahydrate. Acta Crystallographica, 19, 526–543.

Taylor, J.C., Mueller, M.H., and Hitterman, R.L. (1966) Crystal structure of thorium nitrate pentahydrate by neutron diffraction. Acta Crystallographica, 20, 842–851.

Templeton, D.H., Zalkin, A., Ruben, H., and Templeton, L.K. (1985) Redetermination and absolute configuration of sodium uranyl (VI) triacetate. Acta Crystallographica, C41, 1439.

Teo, B.K. (1986) EXAFS: Basic principles and data analysis, 349 p. Springer-Verlag, Berlin.

Teo, B.K., and Lee, P.A. (1979) Ab initio calculations of amplitude and phase functions for extended X-ray absorption fine structure spectroscopy. Journal of the American Chemical Society, 101–11, 2815–2829.

Ueki, T., Zalkin, A., and Templeton, D.H. (1966) Crystal structure of thorium nitrate pentahydrate by X-ray diffraction. Acta Crystallographica, 20, 836–841.

Vance, E.R. (1974) The anomalous optical absorption spectrum of low zircon. Mineralogical Magazine, 39, 709–714.

——— (1975) α-Recoil damage in zircon. Radiation Effects, 24, 1–6.

Vance, E.R., and Anderson, B.W. (1972) Metamict zircons from Ceylan. Mineralogical Magazine, 38, 605–613.

Vance, E.R., and Mackey, D.J. (1974) Optical study of U^{5+} in zircon. Journal of Physics C: Solid State Physics, 7, 1898–1908.

——— (1975) Further studies of the optical absorption spectrum of U^{5+} in zircon. Journal of Physcics C, Solid State Physics, 8, 3439–3447.

Vance, E.R., Efstathiou, L., and Hsu, F.H. (1980) X-ray and positron annihilation studies of radiation damage in natural zircons. Radiation Effects, 52, 61–68.

Wendlandt, W.Wm., and Hecht, H.G. (1966) Reflectance spectroscopy, 298 p. Wiley, New York.

Wyckoff, R.W.G. (1963) Crystal structure, vol. I (2nd edition) 467 p. Wiley, New York.

Yada, K., Tanji, T., and Sunagawa, I. (1981) Applications of lattice imagery to radiation damage investigation in natural zircon. Physics and Chemistry of Minerals, 7, 47–52.

——— (1987) Radiation induced lattice defects in natural zircon ($ZrSiO_4$) observed at atomic resolution. Physics and Chemistry of Minerals, 14, 197–204.

Zimmer, P. (1986) Etude expérimentale, à haute température et haute pression, de système ternaire UO_2-ThO_2-SiO_2 en présence d'une phase fluide. Comparaison avec les systèmes, ZrO_2-ThO_2-SiO_2 et UO_2-ZrO_2-SiO_2. Implications géologiques, 234 p. Mémoire CREGU n°12, Géologie et Géochimie de l'uranium. Thesis (unpublished), CREGU/Université Nancy I, Nancy (in French).

Manuscript received July 4, 1989
Manuscript accepted November 10, 1990